RESEARCH ARTICLE SUMMARY

DRUG DEVELOPMENT

Relocalizing transcriptional kinases to activate apoptosis

Roman C. Sarott†, Sai Gourisankar†, Basel Karim†, Sabin Nettles, Haopeng Yang, Brendan G. Dwyer, Juste M. Simanauskaite, Jason Tse, Hind Abuzaid, Andrey Krokhotin, Tinghu Zhang, Stephen M. Hinshaw, Michael R. Green*, Gerald R. Crabtree*, Nathanael S. Gray*

INTRODUCTION: Protein kinases are central signaling nodes in cells. They control and amplify stimuli from the cell membrane to the nucleus, and they are commonly deregulated in disease. Many cancers rely on kinase mutation or overexpression to sustain aberrant proliferation and survival. Therefore, kinases have been prioritized as drug targets for precision therapies, and extensive drug discovery efforts have given rise to numerous potent inhibitors of kinase catalytic activity. Because of the success of kinase inhibitors in the clinical setting, there is broad interest in expanding the toolset of kinase-targeting modalities.

RATIONALE: Cyclin-dependent kinases (CDKs) that regulate transcription are promising therapeutic targets in cancer. Pharmacological perturbation of transcriptional CDKs using selective small-molecule inhibitors and targeted protein degraders has been investigated. Such molecules phenocopy genetic loss of CDK function and confront mechanism-based toxicity because transcriptional CDKs are essential for healthy cells. Instead of seeking to inhibit or degrade CDKs, we developed a pharmacological strategy that uses chemically induced proximity to convert transcriptional kinases into cancer-specific activators of cell death genes.

RESULTS: We developed bivalent molecules to focus the activity of transcriptional kinases upon the B cell lymphoma 6 (BCL6) transcription factor, the overexpression of which drives diffuse large B cell lymphoma by regulating both cell death and proliferation. The centerpiece of our efforts was a library of compounds that link structurally diverse, ATP-competitive inhibitors of CDK9, a subunit of the positive transcription elongation factor b (P-TEFb) complex, with binders of the BCL6 broad-complex, tramtrack, and bric-à-brac (BTB) domain. We called these molecules CDK-transcriptional/epigenetic chemical inducers of proximity (CDK-TCIPs), and we devised an assay cascade to identify compounds that (i) activate BCL6-regulated transcription, (ii) form ternary complexes with CDK9 and BCL6, and (iii) kill BCL6-overexpressing lymphoma cells. The most potent CDK-TCIPs killed diffuse large B cell lymphoma cells at subnanomolar concentrations 100 times more potently than the combined effect of small molecules that inhibit CDK9 and BCL6. Additionally, these molecules were 200 times less toxic to normal human lymphocytes than they were to diffuse large B cell lymphoma cells.

Our proteomic, epigenomic, and transcriptomic studies indicated that CDK-TCIPs relocalized a fraction of cellular CDK9 to BCL6-bound DNA, overriding the epigenetic silencing that BCL6 ordinarily enforces. At sites where BCL6 was bound, the molecules caused elongation of RNA polymerase II and activation of pro-apoptotic, BCL6-target genes, leading to cell death. The most potent molecule was specifically cytotoxic to BCL6-overexpressing lymphoma cells in a panel of 859 diverse cancer cell lines.

Using our assay cascade, we showed that the concept of relocalizing kinase activity to modulate gene expression extends beyond CDK9 to other transcriptional kinases. CDK-TCIPs linking inhibitors of CDK12 and CDK13 with ligands of BCL6, similarly to CDK9-BCL6 molecules, activated BCL6-regulated transcription and killed lymphoma cells.

We improved the physical and chemical properties of CDK-TCIPs and used them to specifically ablate BCL6-dependent germinal center B cells in a mouse immunization model. Other B cell populations were spared. Our molecules represent a starting point for therapeutic approaches in cancer and autoimmune conditions.

CONCLUSION: Bivalent molecules linking CDK9, CDK12, and CDK13 inhibitors to BCL6 ligands potently and specifically killed BCL6-overexpressing cells. These molecules functioned by relocalizing CDKs to activate cell death gene expression ordinarily repressed by BCL6. Thus, CDK-TCIPs contrast with modalities that kill cancer cells through targeted inhibition or degradation of kinases. Our studies suggest that other potent and selective kinase inhibitors may be used to relocalize kinase activity to induce genes for therapeutic purposes. The gain-of-function mechanism used by CDK-TCIPs could prevent therapeutic relapse due to secondary cancer drivers or alternative oncogenic pathways. ∎
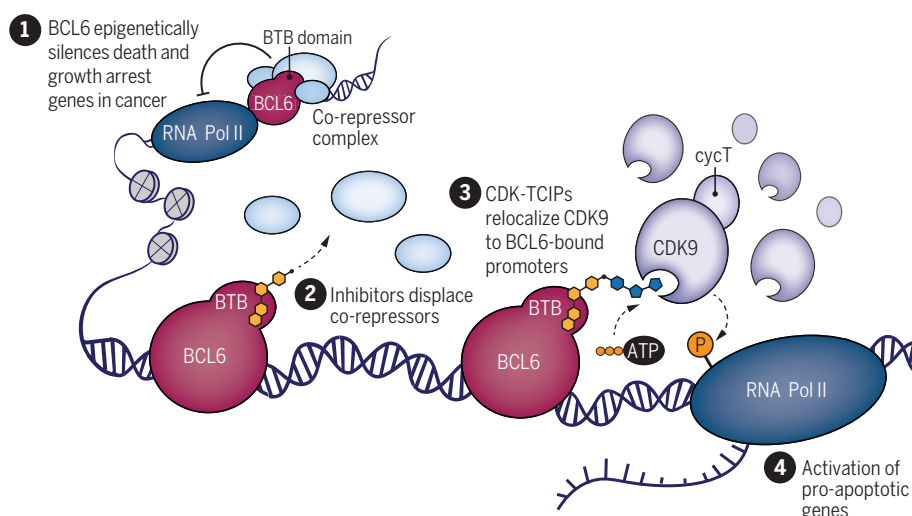
Turning kinase inhibitors into activators of therapeutic genes. The transcription factor BCL6 interacts with epigenetic co-repressors to regulate cell death and proliferation in lymphoma. We linked small molecules that bind to BCL6, displacing its co-repressors, to ligands of the transcriptional kinase CDK9. The resulting bivalent molecules redirected CDK9 and its activity to BCL6-regulated loci, thus activating cell death.

READ THE FULL ARTICLE AT
https://doi.org/10.1126/science.adl5361

RESEARCH ARTICLE

DRUG DEVELOPMENT

Relocalizing transcriptional kinases to activate apoptosis

Roman C. Sarott[1]†, Sai Gourisankar[1]†, Basel Karim[2]†, Sabin Nettles[3], Haopeng Yang[4], Brendan G. Dwyer[1], Juste M. Simanauskaite[3], Jason Tse[1], Hind Abuzaid[3], Andrey Krokhotin[3], Tinghu Zhang[1], Stephen M. Hinshaw[1], Michael R. Green[4]*, Gerald R. Crabtree[3,5]*, Nathanael S. Gray[1]*

Kinases are critical regulators of cellular function that are commonly implicated in the mechanisms underlying disease. Most drugs that target kinases are molecules that inhibit their catalytic activity, but here we used chemically induced proximity to convert kinase inhibitors into activators of therapeutic genes. We synthesized bivalent molecules that link ligands of the transcription factor B cell lymphoma 6 (BCL6) to inhibitors of cyclin-dependent kinases (CDKs). These molecules relocalized CDK9 to BCL6-bound DNA and directed phosphorylation of RNA polymerase II. The resulting expression of pro-apoptotic, BCL6-target genes caused killing of diffuse large B cell lymphoma cells and specific ablation of the BCL6-regulated germinal center response. Genomics and proteomics corroborated a gain-of-function mechanism in which global kinase activity was not inhibited but rather redirected. Thus, kinase inhibitors can be used to context-specifically activate transcription.

Protein kinases have pivotal roles in cellular signaling and are among the most important drug targets ([1]). Many are key regulators of transcription, such as the cyclin-dependent kinases (CDKs) CDK9, CDK12, and CDK13, which function in concert with their cyclin-binding partners to modulate RNA polymerase II (Pol II) activity in the nucleus. CDK9 and cyclin T1, T2, or K form the positive transcription elongation factor b (P-TEFb) complex to enable the release of paused Pol II into elongation by phosphorylation of negative elongation factors and serine 2 (Ser 2) of the Pol II C-terminal domain ([2]). Because many cancers require the transcription of proto-oncogenes such as *MYC* ([3]), potent and specific ATP-competitive inhibitors have been developed to silence the activity of CDK9 and other transcriptional kinases to abolish oncogenic transcription ([4], [5]).

Approaches using chemically induced proximity are promising alternatives to small-molecule inhibitors. Small-molecule chemical inducers of proximity (CIPs) that induce molecular proximity between cellular proteins have been used to recapitulate diverse biological processes in living cells and organisms, including posttranslational modification, signal transduction, and transcrip-

tion ([6]). Among the advantageous features of CIPs is their ability to cause a cellular event with substoichiometric binding of proteins. CIP induction of protein-protein proximity can also be catalytic for a cellular process of interest such as targeted protein degradation ([7]). Indeed, bivalent small molecules called proteolysis-targeting chimeras (PROTACs), which target proteins for degradation by the ubiquitin-proteasome system, rely on chemically induced proximity and have enabled the removal of disease-relevant proteins in the clinical setting, including kinases ([8], [9]). Although mechanistically distinct, both inhibitors and protein degraders phenocopy genetic loss-of-protein function.

We tested whether chemically induced proximity could be used to turn kinase inhibitors into activators of epigenetically silenced transcriptional states. To do so, we focused on the transcription of genes silenced by zinc-finger transcription factor BCL6 (B cell lymphoma 6), which is deregulated and overexpressed in 40 to 60% of cases of human diffuse large B-cell lymphoma (DLBCL), driving the progression of this cancer ([10], [11]). During germinal center (GC) B cell development, BCL6 ordinarily silences the transcription of tumor suppressor and programmed cell death (apoptotic) genes, including *PMAIP1* (phorbol-12-myristate-13-acetate–induced protein 1) or NOXA (Latin for "damage"), *TP53* (tumor protein p53), and *CDKN1B* (cyclin-dependent kinase inhibitor 1B) or p27 ([12]). Target gene silencing is mediated by epigenetic co-repressors such as BCOR (BCL6 co-repressor), NCOR1 (nuclear receptor co-repressor 1), and SMRT (silencing mediator for retinoid and thyroid hormone receptors), which bind to the BCL6 N-terminal BTB (broad-

complex, tramtrack, and bric-à-brac) domain (BCL6^BTB) ([13], [14]). BCL6 acts as an oncogene in DLBCL by suppressing the DNA damage response and cell death pathways. It is deregulated directly by chromosomal translocations and mutations in regulatory regions ([11]) or indirectly by inactivating mutations of antagonistic factors ([15]). Multiple high-affinity inhibitors of BCL6^BTB and BCL6 degraders have been developed but exhibit only small effects on tumor antiproliferation ([16–18]). We and others have previously reported strategies to directly activate gene expression or epigenetic memory by CIP-mediated recruitment of transcriptional activators ([19–22]).

A genome-wide screen for proteins that induce transcription through CIPs detected several kinases ordinarily involved in transcriptional elongation ([23]). Many clinical-stage, small-molecule binders of kinases are available, so we explored whether recruitment of transcription elongation complexes through their kinase subunits to DNA sequences bound by BCL6 might activate BCL6-repressed cell death. We devised a general CIP-based strategy (Fig. 1A) to recruit endogenous CDK9 and other elongation factor kinases to induce the transcription of BCL6-regulated death genes in lymphoma cells. ATP-competitive kinase inhibitors were converted to nanomolar activators of transcription when linked to ligands of BCL6^BTB. Such molecules, called CDK-TCIPs (CDK-transcriptional/epigenetic chemical inducers of proximity), operated by rapid relocalization of a fraction of CDK9, formation of ternary complexes at BCL6-bound loci, induction of Pol II Ser 2 phosphorylation (Pol II Ser 2 phos), and transcription of pro-apoptotic, BCL6-target genes. The cell-killing effect was specific to BCL6-driven cells in both malignant and normal immunological settings. We also illustrate a sequential array of targeted assays to predictably develop gain-of-function CDK-TCIPs to convert seven different clinical-stage kinase inhibitors of CDK9, CDK12, and CDK13 into context-specific inducers of transcription. Collectively, our CDK-TCIP approach highlights a strategy that redirects rather than inhibits kinase activity, with potentially therapeutic effects.

Results

CDK-TCIPs exhibit BCL6-specific cell killing

Reasoning that the proximity of the P-TEFb complex to a promoter would be sufficient for activation of BCL6-target genes (Fig. 1A), we synthesized a library of bivalent molecules in which inhibitors of CDK9 and ligands of the BCL6^BTB were connected through linkers of various lengths and chemical composition (fig. S1A and table S1). A cascade of three critical assays was established to iteratively design and assess CDK-TCIPs by measuring (i) ternary complex formation using purified BCL6^BTB

[1]Department of Chemical and Systems Biology, Stanford University, Stanford, CA 94305, USA. [2]Department of Chemistry, Stanford University, Stanford, CA 94305, USA. [3]Department of Pathology, Stanford University, Stanford, CA 94305, USA. [4]Department of Lymphoma & Myeloma, MD Anderson Cancer Center, Houston, TX 77030, USA. [5]Department of Developmental Biology, Stanford University, Stanford, CA 94305, USA.
*Corresponding author. Email: crabtree@stanford.edu (G.R.C.); nsgray01@stanford.edu (N.S.G.); mgreen5@mdanderson.org (M.R.G.)
†These authors contributed equally to this work.
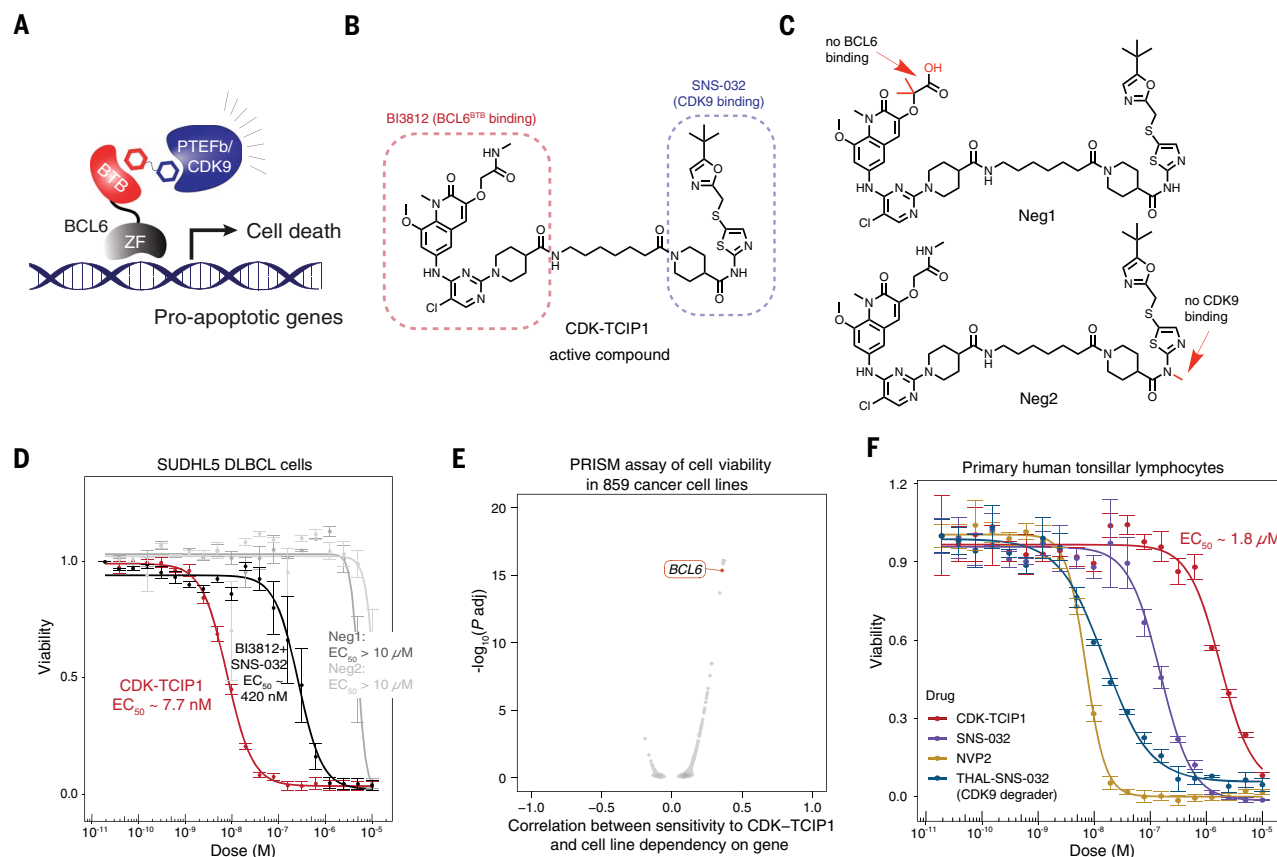
Fig. 1. Development of CDK-TCIPs. (**A**) Schematic of a CDK-TCIP targeting BCL6-regulated loci. (**B**) Structure of lead compound CDK-TCIP1. (**C**) Structures of negative controls containing small chemical modifications abolishing BCL6 binding (Neg1) or CDK9 binding (Neg2). (**D**) Cell-killing potencies of CDK-TCIP1 compared with negative controls and the additive effect of both BCL6 and CDK9 inhibitors combined at 72 hours in SUDHL5 cells. Data are shown as means ± SE. $n = 3$ biological replicates for CDK-TCIP1, Neg1, Neg2, and $n = 2$ biological replicates for BI3812+SNS-032. (**E**) Correlation between genetic dependencies as measured by CRISPR knockout and sensitivity to CDK-TCIP1 among 859 cancer cell lines in PRISM (*61*). (**F**) Toxicity of CDK-TCIP1 (EC$_{50}$ ~1.8 μM) compared with CDK9 inhibitors (SNS-032 EC$_{50}$ ~150 nM, NVP2 EC$_{50}$ ~7.1 nM) or degraders (THAL-SNS-032 EC$_{50}$ ~15 nM) in primary human tonsillar lymphocytes at 72 hours. Data are shown as means ± SD. $n = 2$ biological replicates for CDK-TCIP1 and NVP2, and $n = 1$ with 3 technical replicates for SNS-032 and THAL-SNS-032.

and full-length CDK9/cyclin T1 (CycT1) in a time-resolved fluorescence resonance energy transfer (TR-FRET) experiment, (ii) induction of BCL6-controlled green fluorescent protein (GFP) reporter gene expression, and (iii) viability of high-BCL6-expressing DLBCL cells (fig. S1B).

These studies nominated a lead compound, CDK-TCIP1, which was built using the CDK9 inhibitor SNS-032 (*8, 24*) and BCL6^{BTB}-domain ligand BI3812 (*16*) (Fig. 1B). To evaluate the necessity for both binding moieties of CDK-TCIP1 for biological activity, we synthesized two negative control compounds containing minor chemical modifications to CDK-TCIP1 that abolish binding to either BCL6 (*16*) (Neg1) or CDK9 (Neg2) (Fig. 1C). Neg1 and Neg2 remained comparably strong cell-permeable binders of either CDK9 or BCL6, respectively, as measured by probe-displacement assays inside living cells using nano–bioluminescence resonance energy transfer [nanoBRET (*25*)] between tagged, full-length CDK9-CycT and BCL6 constructs (fig. S2, A and B).

In DLBCL cell lines dependent on high BCL6 expression, such as SUDHL5 (Stanford University-Diffuse Histiocytic Lymphoma-5) with 301 BCL6 transcripts per million (*26*), CDK-TCIP1 had a potent cell-killing effect, with a mean effective concentration (EC$_{50}$) of 7.7 nM in a 72-hour cell-viability assay (Fig. 1D). The cytotoxicity of CDK-TCIP1 was ~55 times greater than the additive effect of the CDK9 and BCL6 parental inhibitors and >10,000 times greater than the additive effect of negative controls (Fig. 1D). In an analysis of 859 different cancer cell lines, CDK-TCIP1 was uniquely potent in DLBCL lines dependent on having high levels of BCL6 expression due to oncogenic mutations in the BCL6 gene or its regulatory regions such as those described in (*11*), indicating a requirement of BCL6 for CDK-TCIP1 potency (Fig. 1E and fig. S3, A and B). CDK-TCIP1 was more specific to BCL6-expressing DLBCL cells than a BCL6-directed bivalent compound designed using inhibitors of BRD4 (fig. S3C) (*19*). In primary T and B lymphocytes taken from human tonsils, CDK-TCIP1 was 200 times less

cytotoxic than in SUDHL5 DLBCL cells. This contrasted with optimized CDK9 degraders and inhibitors, which broadly inhibit transcription (*8*) and are similarly potent in both primary lymphocytes and DLBCL cells (Fig. 1F and fig. S2D). Our results indicate that the CDK-TCIP strategy delivers cancer cell–specific effects and overcomes the on-target toxicity associated with inhibition or degradation of essential kinases, potentially enabling a therapeutic window.

CDK-TCIP1 activity depends on ternary complex formation

Titration of the BCL6^{BTB} inhibitor BI3812 or the CDK9 inhibitor SNS-032 against constant, lethal CDK-TCIP1 doses impaired the cell-killing effect, indicating a requirement for concomitant engagement of CDK9 and BCL6 for the observed cytotoxicity (fig. S2C). Therefore, we hypothesized that ternary complex formation between CDK9 and BCL6 is necessary for cell killing through the induction of BCL6-target genes. Among the synthesized compounds, bivalent

molecules incorporating the CDK9 inhibitor SNS-032 exhibited the most consistent structure-activity relationship between ternary complex formation in vitro and DLBCL cell–killing potency (Fig. 2A). In addition, for molecules prepared using five different CDK9 inhibitors, we observed that the formation of ternary complexes in vitro and in cells was a prerequisite for the expression of BCL6-controlled GFP in SUDHL5 cells (table S1 and fig. S4, A and B).

The lead molecule, CDK-TCIP1, formed a ternary complex between purified BCL6[BTB] and

CDK9-CycT1, with an EC_{50} of 11 nM (fig. S5A), and activated BCL6-controlled GFP expression in DLBCL cells, with a comparable EC_{50} of 58 nM (Fig. 2B). In human embryonic kidney SV40 large T antigen transformed (HEK293T) cells, which do not contain endogenous BCL6, CDK-TCIP1 formed a ternary complex between overexpressed full-length CDK9 and full-length BCL6 constructs with a EC_{50} of 22 nM as measured by a nanoBRET assay (fig. S5B). In almost all assays we observed a bell-shaped curve characteristic of the saturation behavior of bivalent

molecules at high concentrations (6). Neg1 and Neg2 had negligible effects in the transcriptional activation reporter and ternary complex formation assays at comparable doses, demonstrating the requirement for dual binding of CDK9 and BCL6. Collectively, these studies support the necessity of formation of a transcription-competent ternary complex that is critical for CDK-TCIP1–mediated DLBCL cell killing.

To evaluate the direct effect on endogenous proteins with CDK-TCIP1 in an unbiased manner, we performed global proteome profiling
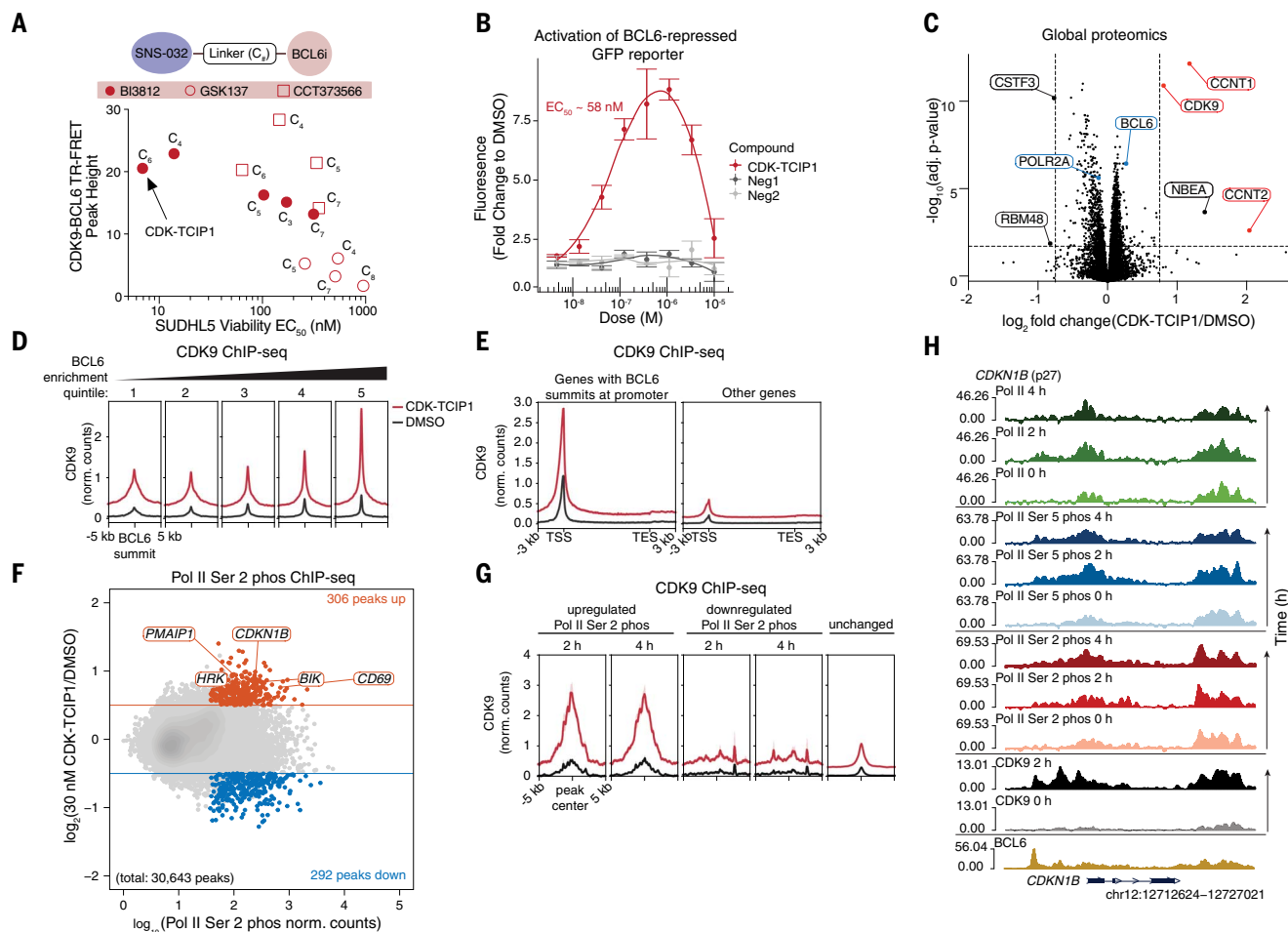
Fig. 2. CDK-TCIP1 functions by ternary complex formation and relocalization of CDK9 activity to BCL6 on chromatin. (**A**) Correlation of ternary complex formation with cell-killing potency (72 hours in SUDHL5 cells) for CDK-TCIPs constructed from the CDK9 inhibitor SNS-032 and three different BCL6[BTB] inhibitors. The adjacent "C#" denominates the number of carbon atoms in the linear alkyl linker. Points represent a mean of $n = 3$ technical replicates for TR-FRET. (**B**) Activation of BCL6-repressed GFP reporter construct integrated into KARPAS422 cells after compound treatment for 24 hours. Data are shown as means ± SD. $n = 3$ biological replicates. (**C**) Whole-proteome profiling of SUDHL5 cells treated with 30 nM CDK-TCIP1 for 2 hours plotted with cutoffs of |log$_2$(fold change)| ≥ 0.75 and adjusted $P ≤ 0.01$ using a moderated t test and Benjamini-Hochberg adjustment. $n = 4$ biological replicates. (**D**) ChIP-seq measurement of CDK9 at BCL6 summits genome wide after 30 nM CDK-TCIP1 treatment for 2 hours in SUDHL5 cells. Summits of BCL6 enrichment computed from peaks were reconstructed from ChIP-seq in (62). (**E**) ChIP-seq measurement of CDK9

to genes that have BCL6 summits at their promoters. (**F**) Changes in local RNA Pol II Ser 2 phosphorylation as measured by ChIP-seq after 2 hours of 30 nM CDK-TCIP1 addition in SUDHL5 cells; colors indicate adjusted $P ≤ 0.05$ and |log$_2$(drug/DMSO)| ≥ 0.5, $n = 2$ biological replicates. P values were computed by two-sided Wald test and adjusted for multiple comparisons using the Benjamini-Hochberg procedure. Labeled are known BCL6-target, cell cycle arrest, and pro-apoptotic genes. (**G**) ChIP-seq measurement of CDK9 after 30 nM CDK-TCIP1 treatment for 2 hours at differentially induced Pol II Ser 2 phos peaks classified in (F). (**H**) ChIP-seq tracks of CDK9, Pol II Ser 2 phos, Pol II Ser 5 phos, and Pol II at the BCL6-target gene *CDKN1B*. In (D), (E), and (G), hours, metaprofiles, and tracks for CDK9 measured with Abcam's ab239364 anti-CDK9 antibody are shown with two biological replicates merged, spike-in normalized, and input subtracted. For Pol II Ser 2 phos and Pol II Ser 5 phos, two biological replicates were merged, sequence-depth normalized, and input subtracted. For Pol II, three biological replicates were merged, sequence-depth normalized, and input subtracted. The BCL6 track is from (62).

by treating the DLBCL cell line SUDHL5 with 30 nM CDK-TCIP1, Neg1, and Neg2 for 2 hours, followed by protein digestion and liquid chromatography–tandem mass spectrometry analysis of peptides using data-independent acquisition parallel accumulation serial fragmentation, which quantified 169,000 peptides and 8100 unique proteins on average. Unlike the case for Neg1 or Neg2 treatment, CDK-TCIP1 increased the abundance of cyclin T1 (CCNT1; >2-fold) and T2 (CCNT2; >2-fold), CDK9 (1.8-fold), and BCL6 (1.2-fold), with negligible changes to other proteins (>2-fold) above the statistical cutoff (adjusted P value = 0.05; Fig. 2C; fig. S6, A to C; and table S3). Given the short treatment time and unchanged mRNA abundance of these highlighted proteins (Fig. 3C), these changes in abundance are unlikely to occur through induced transcription. Instead, the data support thermodynamic stabilization or protection from proteasomal degradation of the BCL6–P-TEFb complex by CDK-TCIP1.

Induced proximity of CDK9 is sufficient to induce transcription

To assess the functional importance of recruited CDK9 catalytic activity, we constructed a synthetic CIP system by overexpressing FK506-binding protein 12 with a phenylalanine 12-to-valine mutation (FKBP^{F36V})–tagged wild-type (WT) or mutant CDK9 in our BCL6-controlled GFP reporter cell line (fig. S7, A and C). We then synthesized a cell-permeable bivalent compound, RCS-03-207, which linked a synthetic ligand of FKBP^{F36V} (o-AP1867) with the BCL6^{BTB}-domain binder BI3812 (fig. S7, B and D). In this model system, RCS-03-207 treatment produced a dose-dependent increase in GFP for fused constructs containing WT and a substantially reduced response for catalytically inactive D167N (27) mutant CDK9 (fig. S7E). The modest GFP signal detected in the catalytically inactive CDK9 condition suggests that there may be a minor contribution from co-recruitment of additional copies of P-TEFb. However, CDK9 was reportedly inactive in the dimeric form (28). Overexpression of the WT CDK9-FKBP^{F36V} construct further potentiated GFP transcription after CDK-TCIP1 treatment relative to endogenous CDK9 levels and had a characteristic hook effect (fig. S7F).

Recruitment of enzymatically functional, active CDK9 is thus likely a requirement for CDK-TCIP–dependent transcriptional activation of BCL6 gene loci. Given a diffusion-limited rate constant of ~10^8 M^{-1} s^{-1} and the ternary binding apparent EC$_{50}$ of CDK-TCIP1 of ~22 nM inside the cell (fig. S5B), the off rate of
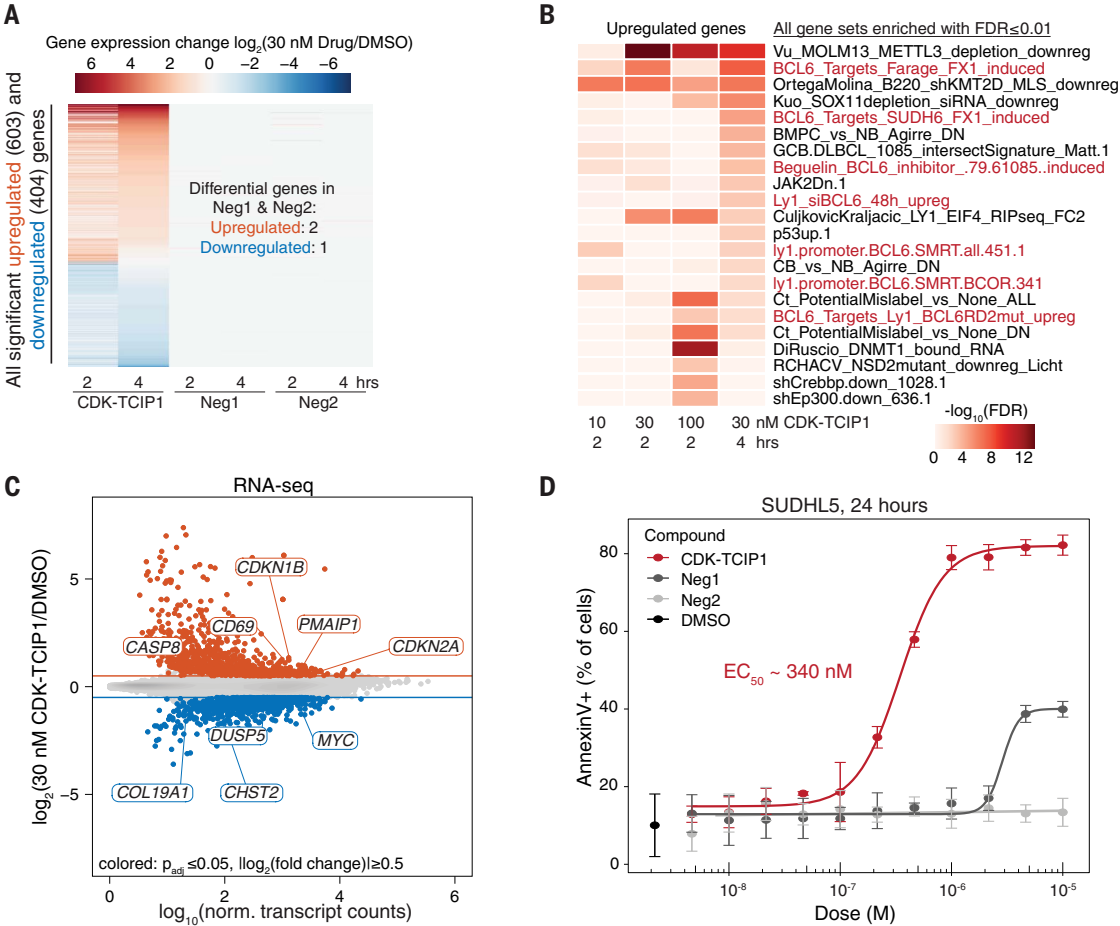
Fig. 3. Activation of apoptotic signaling. (**A**) Time-dependent changes in gene expression measured by mRNA sequencing after 30 nM CDK-TCIP1 addition in SUDHL5 cells compared with controls. Plotted are differential genes with adjusted $P \leq 0.05$ and $|\log_2$(fold change)$| \geq 1$. $n = 3$ to 4 biological replicates. P values were computed by two-sided Wald test and adjusted for multiple comparisons using the Benjamini-Hochberg procedure. (**B**) Gene expression programs enriched in up-regulated genes (adjusted $P \leq 0.05$, fold change ≥ 1.5) at each time point defined from (A). P value of enrichment was computed by hypergeometric test and adjusted for multiple comparisons using the Benjamini-Hochberg procedure for FDR. (**C**) Acute effects on gene expression and known BCL6-target genes (labeled) caused by the addition of 30 nM CDK-TCIP1 for 2 hours. $n = 3$ to 4 biological replicates. P values were computed by two-sided Wald test and adjusted for multiple comparisons using the Benjamini-Hochberg procedure. (**D**) Dose-dependent apoptosis in SUDHL5 cells measured by annexin V staining after 24 hours of compound. $n = 3$ biological replicates. Data are shown as means ± SD.

ternary complex formation is ~2.2 s^{-1}, similar to rates of ADP release from kinase active sites (29–31). Therefore, the CDK-TCIP1 ternary complex should fall apart frequently enough (about once every 0.45 s) to permit catalytic activity at BCL6-bound loci. We propose a potential "catch-and-release" mechanism whereby CDK-TCIP1 recruits and subsequently releases catalytically active CDK9 to BCL6 loci for transcriptional activation of BCL6-repressed genes (fig. S7G). Such a model could also explain a recent study of bivalent molecules that recruited histone deacetylase activity through a substrate-competitive inhibitor (32).

Relocalization of CDK9 activity to BCL6 targets on chromatin

To define the direct effects of CDK-TCIP1 on CDK9 localization and activity on chromatin, we conducted chromatin immunoprecipitation followed by next-generation sequencing (ChIP-seq) of CDK9 in DLBCL cells treated with 30 nM CDK-TCIP1 at an early time point (2 hours) using spiked *Drosophila melanogaster* chromatin to enable normalization and quantification of absolute changes in CDK9 levels. At this concentration, the percentage of total CDK9 or BCL6 engaged in the cell was far less than their respective inhibitors, as evidenced by the nanoBRET probe displacement assays shown in fig. S2, A and B. Approximately 10,000 CDK9 peaks were reconstructed in SUDHL5 and in KARPAS422 [established by Karpas and colleagues (33)] DLBCL cell lines, as detected with two different antibodies to CDK9, with a strong correlation between biological replicates and with most of the variance being driven by CDK-TCIP1 treatment (fig. S8, A to C). CDK-TCIP caused rapid and robust recruitment of CDK to BCL6-binding sites (see the materials and methods) on chromatin in both SUDHL5 and KARPAS422 cells (Fig. 2D and fig. S8, D and E). The increased local amounts of CDK9 correlated with increasing BCL6 enrichment, corroborating BCL6-dependent recruitment on chromatin. Genes with high-confidence BCL6-binding summits within 3 kilobases of their transcription start sites (TSS) at their promoters showed three times greater CDK9 at both the promoter and across the gene body, whereas other genes had negligible changes over background (Fig. 2E and fig. S8, F and G). CDK9 was recruited to both promoters and enhancers with BCL6 summits; regions without BCL6 showed modest increases or no changes in CDK9 occupancy (fig. S8H). In SUDHL5 cells, five times as many peaks increased (604, 5.1% of all 11,716 peaks) in CDK9 binding as decreased (142, 1.2% of all 11,716 peaks), as calculated by differential peak analyses using relative log expression normalization (fig. S8I). This is consistent with global proteomics results indicating stabilization of CDK9 protein in Fig. 2C. The results of these analyses

indicate that CDK9 is rapidly and specifically recruited to BCL6-bound chromatin.

To define the immediate consequences of relocalizing CDK9 to BCL6-bound loci on chromatin, we characterized changes in Pol II and the phosphorylation of its C-terminal domain at Ser 2 and Ser 5 by ChIP-seq at 2 and 4 hours after CDK-TCIP1 addition (30 nM; fig. S9A). A select number of Pol II Ser 2 phosphorylation peaks were induced, primarily at promoters (306 peaks up, adjusted $P \leq 0.05$, and fold change ≥ 1.4; Fig. 2F and fig. S9B). Peaks that increased in Pol II Ser 2 phos at 2 and 4 hours were enriched for compound-induced CDK9 binding, whereas those that decreased or remained unchanged had negligible changes in CDK9 levels (Fig. 2G). Among the most induced Pol II Ser 2 phos sites were known BCL6-repressed cell death and tumor-suppressor genes such as *PMAIP1*, *BIK* (BCL2-interacting killer), *HRK* (Harakiri), and *CDKN2B* (Fig. 2, F and H, and fig. S8H). Induced peaks were significantly (adjusted $P < 0.0001$) enriched at sites identified as bound by components of the BCL6:Polycomb Repressive Complex 1 (PRC1) epigenetic repressor complex [BCL6, BCOR, and KDM2B (34, 35)], as analyzed in public ChIP-seq datasets from >6500 blood cell lines (fig. S9C). This is consistent with the observation that CDK9 is recruited to BCL6 sites, as shown in Fig. 2, D and E. A peak-to-gene analysis using GREAT (Genomic Regions Enrichment of Annotations Tool) (36) confirmed that these induced peaks occurred near genes related to pathways repressed by BCL6, including programmed cell death and cell cycle arrest biological processes [false discovery rate (FDR) < 0.01] (fig. S9D). Loci that showed decreased Pol II Ser 2 phosphorylation (292 peaks down, adjusted $P \leq 0.05$, and fold change ≤ -1.4; Fig. 2F) corresponded with some known BCL6-regulated pathways such as the humoral immune responses (fig. S9D), but had lower enrichment of BCL6 (fig. S9E) and less overlap with BCL6 peaks (fig. S9F) compared with induced Pol II Ser 2 peaks, indicating that decreased peaks may be off-target or indirect effects. These results provide evidence that CDK-TCIPs selectively recruit CDK9 and its activity to BCL6-repressed genetic loci.

Consistent with a mechanism of locus-specific activity, a 4-hour CDK-TCIP1 treatment did not globally alter Pol II Ser 2 phosphorylation or BCL6, CDK9, or Pol II protein abundance, as determined by immunoblotting unless concentrations 10 times greater than the cell-killing EC$_{50}$ were applied (fig. S10A), which was consistent with global proteome profiling (Fig. 1G) and nanoBRET displacement data (fig. S2, A and B). There was little change in total Pol II abundance at either genes with BCL6 sites at their transcription start sites or elsewhere (fig. S9G). Our data support a gain-of-function mechanism in which CDK-TCIP1

relocalizes a fraction of cellular CDK9 to BCL6-bound loci.

Activation of BCL6-target gene expression and apoptotic signaling

Transcriptome analysis by RNA sequencing after short treatments (2 or 4 hours) in SUDHL5 cells of CDK-TCIP1 (10, 30, or 100 nM) identified a set of 603 genes that showed significantly increased transcription (adjusted $P \leq 0.05$ and fold change ≥ 2) and fewer ($n = 404$) that decreased in expression (Fig. 3A). Genes with increased transcription were enriched for multiple annotated BCL6-target gene sets (Fig. 3B). Gene expression changes and enrichment for BCL6 signaling were dose dependent (fig. S11A).

CDK-TCIP1 increased the expression of proapoptotic, BH3 (BCL2 homology 3)-domain containing, BCL6-target genes in mRNA, including *BBC3* (BCL2-interacting protein 3; also called PUMA for p53-upregulated modulator of apoptosis) and *PMAIP1* (also called NOXA), as well as the cell cycle arrest gene *CDKN1B* (p27) significantly (adjusted $P \leq 0.05$), by more than 1.6 times over DMSO control (Fig. 3C and fig. S11, B to D). In addition, mRNA for two other pro-apoptotic genes, *BAX* (BCL2-associated X, apoptosis regulator) and *BIM* (BCL2-interacting mediator of cell death; also called *BCL2L11* for BCL2 like 11), showed statistically significant, modest increases of 1.2 times over control. The anti-apoptotic *MCL1* (myeloid cell leukemia sequence 1) also increased by 20%. These genes also displayed recruitment of CDK9 and increased Pol II Ser 2 phosphorylation (Fig. 2, F and H). Induction of some of these targets at the protein level was observed in two different cell lines (SUDHL5 and KARPAS422) but was muted in magnitude (fig. S11 and global proteomics at 2 hours in table S3). The small increase in the BH3-only protein PUMA, which is required for p53-mediated cell death (37), was concurrent with an increase in NOXA, another BH3-only protein (fig. S11). BH3-only proteins act cumulatively to initiate cell death (38). These observations may suggest that an excess of BH3-domain–containing, proapoptotic proteins over anti-apoptotic proteins may be responsible for cell death. For p27, induction was small and delayed (fig. S11, B to D), indicating that the increase reflects a cell cycle block, and that the rapid (at 2 hours) increase in Ser 2 phosphorylation along its gene body (Fig. 2, F and H) and gene expression (Fig. 3C) could reflect other regulatory mechanisms.

Annexin V staining after 24 hours showed that CDK-TCIP1 induced dose-dependent apoptosis in SUDHL5 cells with an EC$_{50}$ of 340 nM (Fig. 3D). By contrast, 10 to 1000 times greater concentrations of negative controls Neg1 and Neg2 were required for effects in this assay, consistent with their negligible effects on gene transcription (Fig. 3D). Thus, CDK-TCIP1

activates death pathways repressed by BCL6, consistent with the rational optimization of the compound to induce BCL6-repressed transcription, as shown in Figs. 1 and 2.

An investigation into transcripts decreasing after treatment of cells with CDK-TCIP1 (30 nM) revealed that these were genes associated with GC B cell programs, for which BCL6 is a master regulator (fig. S12A). *BCL6* itself, which contains a BCL6-binding site in its first intron and is auto-regulated (*39*), showed a small decrease in Pol II Ser 2 phosphorylation and increase in CDK9, Pol II, and Pol II Ser 5 phosphorylation at its promoter, suggesting initiated but paused Pol II (fig. S12B). *BCL6* expression decreased by ~12% (adjusted $P = 0.003$) 4 hours after treatment with CDK-TCIP1 (30 nM), but showed no change in protein level at this time point and dose (fig. S10A). The increase in CDK9 at these and other loci, which nonetheless decrease in marks associated with transcriptional elongation, may reflect non-canonical roles of CDK9 in silencing gene expression, such as those described in (*40*).

Rational chemical optimization of CDK-TCIPs

We used medicinal chemistry to design CDK-TCIPs with improved physicochemical properties and increased potency compared with CDK-TCIP1, which exhibited poor pharmacokinetic properties that precluded further preclinical drug development (fig. S13, A and B). Inspired by optimization studies of protein-degrader drug candidates (*41, 42*), we focused on introducing rigid, amine-containing linkers to replace the flexible *n*-hexyl (C_6) chain in CDK-TCIP1 (fig. S14A). These studies identified several compounds that exhibited enhanced ternary complex formation, activation of BCL6-controlled transcription, and cell killing (fig. S14, A to F).

We synthesized several versions of CDK-TCIPs, and CDK-TCIP2, which incorporates a rigid 3,9-diazaspiro[5.5]undecyl linker motif, emerged as a new, more potent compound that killed SUDHL5 cells at subnanomolar concentrations ($EC_{50} = 0.9$ nM; fig. S14C). In mice, CDK-TCIP2 exhibited improved metabolic stability and higher concentrations in blood than CDK-TCIP1 after intraperitoneal dosing, permitting its use in vivo (area under the curve = 1.4 μM h; fig. S15, A and B). Drug accumulation was ~100 times greater than cellular EC_{50}s, predominantly in the liver, kidney, and spleen (fig. S15C). Our studies demonstrate that CDK-TCIPs are amenable to rational optimization of potency and physicochemical properties through medicinal chemistry and underline the utility of our new TCIP design cascade.

Specific ablation of the GC response in immunized mice

In normal physiology, BCL6 is the master regulator of the GC reaction that is required for T cell–dependent antibody affinity maturation (*43, 44*). The BCL6 protein is highly expressed in GC B cells and T follicular helper cells (*45*) and is down-regulated as cells exit GCs and become memory B cells or plasma cells (*43*). The GC B cell is the counterpart to follicular lymphoma, Burkitt's lymphoma, and the GC B cell–like subtype of DLBCL, which collectively make up >40% of B cell malignancies (*46*). Given the BCL6-targeted, specific effects on transcription and apoptosis in DLBCL cell lines, we investigated whether CDK-TCIP2 might specifically suppress the proliferation of GC B cells in a mouse immunization model.

Two days after immunization of C57BL/6 mice with the T cell–dependent antigen, sheep red blood cells, to stimulate the GC reaction, we began administering CDK-TCIP2 at 5 mg/kg once daily, 10 mg/kg once daily, 5 mg/kg twice daily, or vehicle alone twice daily by intraperitoneal injection. Ten days after immunization, at the peak of the GC reaction, the mice were euthanized and their spleens were collected for flow cytometry of GC B cell populations. GCs were more abundant in vehicle-treated mice, and the percentage of splenic GC B cells ($B220^+Fas^+GL7^+$) was significantly decreased in CDK-TCIP2–treated mice (Fig. 4B). The reduction was dose dependent and highest in the 5 mg/kg twice-daily dosing regimen, likely due to the ~3.2-hour half-life (fig. S15, A and B) of the molecule. The total frequency of $B220^+$ B cells was slightly decreased, commensurate with the loss GC B cells and supporting on-target specificity for the $BCL6^+$ GC B cell compartment (Fig. 4C). A small but statistically insignificant increase in memory B cell abundance was noted, likely reflecting the shunting of B cells out of the GC reaction after its establishment in the first 2 days after immunization but before treatment (Fig. 4D). The compound was well tolerated, with no changes in body weight or other adverse effects observed over the 8-day dosing period (Fig. 4E). These data are consistent with studies showing that although $BCL6^{-/-}$ mice die within weeks of birth from a lethal inflammatory reaction (*47*), mice carrying mutations in the regions of the BCL6 protein that bind its co-repressors have normal lifespans in controlled conditions but exhibit a defect in their ability to form GCs (*48, 49*). These results indicate that CDK-TCIP2 specifically inhibits immunological processes ordinarily facilitated by the repressive function of BCL6 and provide evidence of target engagement in an in vivo setting.

Extension of the CDK-TCIP concept to CDK12 and CDK13

We explored the predictability of our strategy to redirect kinase activity by developing molecules that recruit the transcriptional kinases CDK12 and CDK13 (Fig. 5A), which, similarly to CDK9, phosphorylate Pol II Ser 2 and con-tribute to transcriptional elongation (*50, 51*). In some cancers, CDK12 and CDK13 are deregulated by amplification or mutations (*52, 53*). We synthesized CDK-TCIP3, a molecule that links a potent and selective inhibitor of CDK12 and CDK13 (*54*), with the $BCL6^{BTB}$ ligand BI3812 (Fig. 5B). CDK-TCIP3 exhibited five times higher affinity for CDK12 and CDK13 compared with CDK9 (CDK13-CycK IC_{50} ~65 nM, CDK9-CycT1 IC_{50} ~261 nM) and potently increased the expression of BCL6-repressed GFP, exhibiting the characteristic bell-shaped curve characteristic of CIP function (Fig. 5C). CDK-TCIP3 exhibited a cell-killing effect with an EC_{50} of ~609 nM in SUDHL5 cells after 72 hours of treatment, more than 10 times greater than the effect of the inhibitor of CDK12 and CDK13 alone in these cells (Fig. 5D). These studies suggest that inhibitors of transcriptional kinases beyond CDK9 can be rationally converted into activators of cell death.

Discussion

Kinases control and amplify signals from the cell membrane to the nucleus and are commonly dysregulated in disease. Extensive drug discovery efforts have focused particularly on kinases that are aberrantly activated by mutation or the biochemical actions of cancer drivers. Altogether, more than 50 of the 500 human kinases have been targeted with potent and relatively specific inhibitors for the treatment of cancer, most of which are ATP-competitive, reversible small molecules (*1*).

Transcriptional deregulation is a hallmark of malignant transformation. Thus, many inhibitors of transcriptional kinases (and other nuclear transcriptional regulators) have been optimized for potency, specificity, and physicochemical properties. On-target, mechanism-based toxicities constrain clinical application of the inhibitors, largely due to the need for near-complete inhibition of kinase activity for anti-tumor efficacy (*55*). Recently, many groups have sought to convert inhibitors into selective protein degraders by chemical linking to E3 ligase–binding moieties (*8*). Both inhibitors and protein degraders fundamentally aim to phenocopy genetic loss of aberrant protein function.

We developed CDK-TCIPs, a chemically induced proximity-based gain-of-function strategy, to activate apoptosis by relocalizing transcriptional kinase activity to pro-apoptotic gene loci bound by an overexpressed, oncogenic transcription factor, BCL6. These bivalent molecules function by recruiting elongation kinase activity, as evidenced by the locus-specific recruitment of CDK9 and the induction of Pol II Ser 2 phosphorylation on chromatin. CDK-TCIPs increase the expression of tumor suppressors and pro-apoptotic proteins at low-nanomolar drug concentrations that do not inhibit overall CDK9 kinase activity. The ensuing killing effect
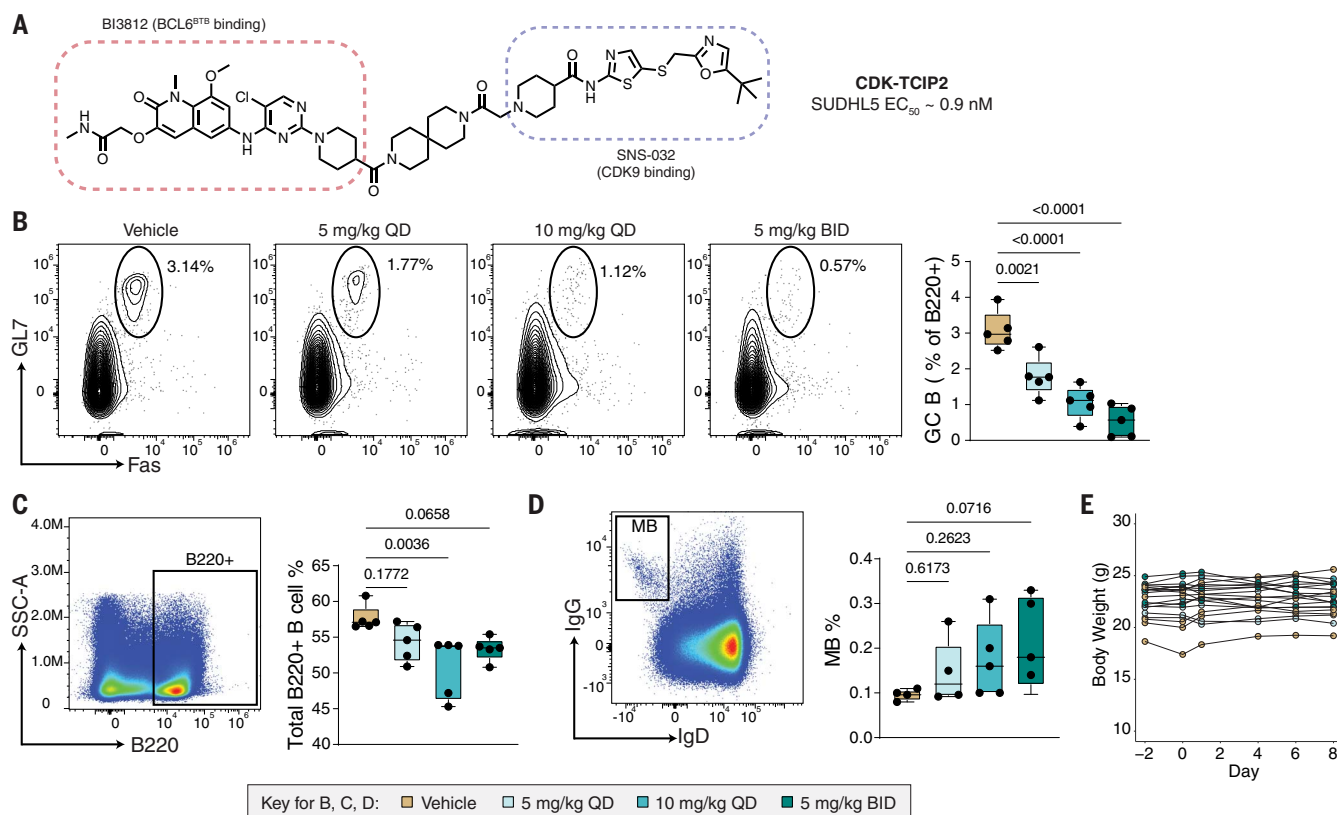
Fig. 4. Ablation of GC B cells in immunized mice. (**A**) Structure of CDK-TCIP2. (**B**) Dose-dependent change in percentage of splenic GC (B220$^+$Fas$^+$GL7$^+$) B cells. (**C**) Change in total frequency of splenic B220$^+$ B cells. (**D**) Change in total frequency of splenic memory B cells (MB). In (B) to (D), representative flow cytometry is shown on the left and quantification on the right from five biological replicates (five different mice) for each condition, median, and range shown. *P* values were computed by unpaired Student's *t* test. QD, once daily; BID, twice daily. Vehicle was given twice daily. (**E**) Body weight changes over time.

is lineage specific to only those cells driven by BCL6 in both malignant cell lines and mouse models of B cell development. This contrasts with CDK9 inhibitors and degraders, which are more broadly cytotoxic to both normal and malignant cells. Our approach thus offers an alternative to conventional chemotherapeutic approaches in oncology that phenocopy genetic or enzymatic loss-of-function effects. Our experiments studying the effect of CDK-TCIPs on the GC also suggest that they may also be useful in rare autoimmune conditions such as systemic lupus erythematosus, which are characterized by the accumulation of autoantibodies acquired during an increased GC response (*56*, *57*). Bivalent molecules have previously been developed to redirect the catalytic activity of kinases to new substrates, demonstrating the roles of proximity and orientation in kinase activation (*58*, *59*). To the best of our knowledge, our work represents the first example of rewiring endogenous kinase activity to drive a therapeutically relevant phenotype in vivo.

We used our assay cascade for rational improvement of CDK-TCIP physicochemical properties and for the discovery of CDK12- and CDK13-targeting CDK-TCIPs, demonstrating the generality of the strategy discovery of CDK12-

and CDK13-targeting CDK-TCIPs, demonstrating the generality of the strategy. Our work indicates that the many targeted and highly optimized kinase inhibitors might be leveraged for the design of therapeutic CIPs that relocalize kinase activity. These molecules would be designed to turn on preexisting but silent cellular signaling pathways such that altered transcription of even a single gene produces a therapeutic effect rather than to silence aberrant catalytic activity. In these applications, specificity would emerge from the programmatic nature of the hijacked transcription factor. The potential of gain-of-function kinase CIPs might extend beyond the induction of programmed cell death pathways to, for example, the activation of differentiation or pluripotency for applications in regenerative medicine or the attenuation of inflammatory signaling.

Methods summary

Full details of the methods are provided in the supplementary materials. Briefly, CDK-TCIP library synthesis was conducted using six different ATP-competitive CDK9 inhibitors and established amide bond formation chemistry. The final compounds were purified by

preparative reverse-phase high performance liquid chromatography and assayed at >95% purity. Transcriptional activation was measured using flow cytometry of KARPAS422 DLBCL cells transduced with a BCL6-driven GFP reporter construct (*19*) and treated with compound. Ternary complex formation was assessed using a biochemical TR-FRET assay with full-length CDK9/CycT and BCL6^{BTB} and an intracellular nanoBRET assay in HEK293T cells with full-length CDK9 and full-length BCL6. Effects on cell viability were determined using a resazurin-based indicator dye after 72 hours of drug treatment. The PRISM cell proliferation assay assessed compound effects after 120 hours and was performed at the Broad Institute (*60*). Mechanistic studies, which included Western blot; annexin staining; and transcriptomic, epigenetic, and proteomic studies, assessed CDK-TCIP effects in DLBCL cells plated at 1 million cells/ml. mRNA sequencing was performed with polyA-enriched transcripts prepared as paired-end libraries. ChIP sequencing was performed with DNA enriched after chromatin immunoprecipitation from formaldehyde–cross-linked cells prepared as paired-end libraries. Global proteomic profiling was performed with peptides from
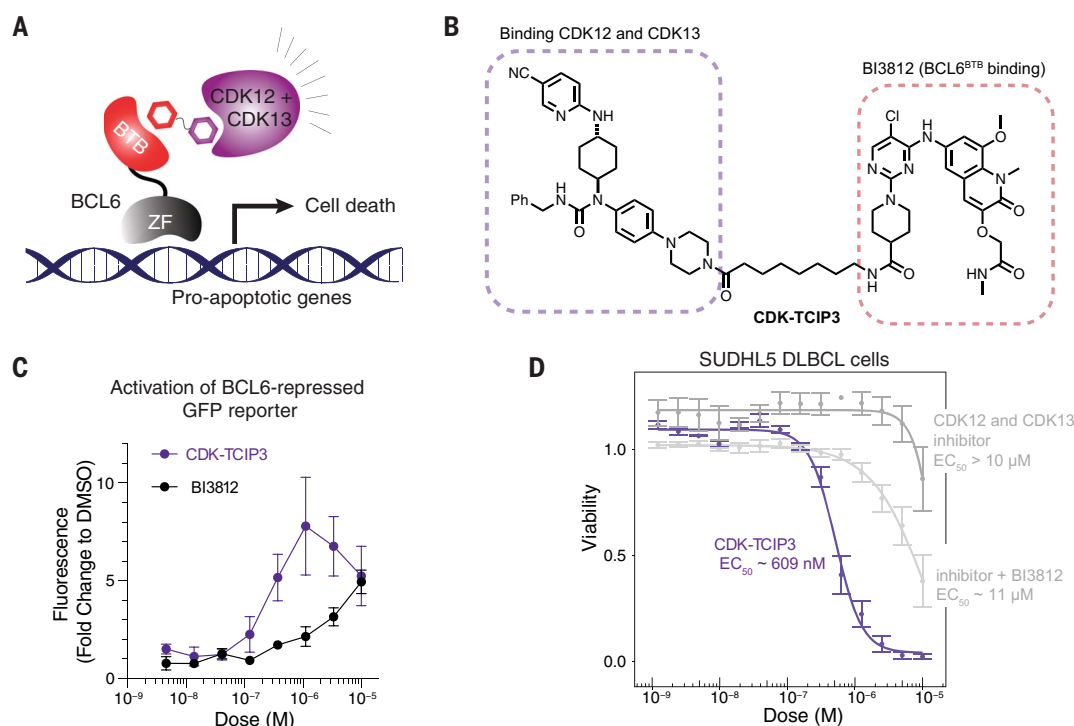
Fig. 5. Extension of the CDK-TCIP concept to CDK12 and CDK13. (**A**) Schematic of recruiting CDK12 and CDK13 to BCL6-bound loci. (**B**) Structure of CDK-TCIP3. (**C**) Activation of BCL6-repressed GFP reporter constructs after 24 hours of compound addition to lymphoma cells. Data are shown as means ± SD. $n = 4$ biological replicates. (**D**) Comparison of cell-killing potency in DLBCL cells at 72 hours between CDK-TCIP3 and the additive effect of both BCL6 and CDK12/13 inhibitors. $n = 3$ biological replicates. Data are shown as means ± SE.

compound-treated cells eluted with a nano-Elute 2 coupled to a timsTOF HT (Bruker). For experiments studying the effect on GCs, C57BL/6 mice were immunized with sheep red blood cells to induce GC formation. Treatment with compound or vehicle by daily intraperitoneal injection started 2 days after immunization. After 8 days of treatment, mice were sacrificed, spleens were homogenized, and cells were analyzed by flow cytometry. Pharmacokinetics of CDK-TCIPs were assessed in C57BL/6 mice by intraperitoneal compound injection.

REFERENCES AND NOTES

1. P. Cohen, D. Cross, P. A. Jänne, Kinase drug discovery 20 years after imatinib: Progress and future directions. *Nat. Rev. Drug Discov.* **20**, 551–569 (2021). doi: 10.1038/s41573-021-00195-4; pmid: 34002056

2. K. Adelman, J. T. Lis, Promoter-proximal pausing of RNA polymerase II: Emerging roles in metazoans. *Nat. Rev. Genet.* **13**, 720–731 (2012). doi: 10.1038/nrg3293; pmid: 22986266

3. J. E. Bradner, D. Hnisz, R. A. Young, Transcriptional addiction in cancer. *Cell* **168**, 629–643 (2017). doi: 10.1016/j.cell.2016.12.013; pmid: 28187285

4. T. A. Constantin, K. K. Greenland, A. Varela-Carver, C. L. Bevan, Transcription associated cyclin-dependent kinases as therapeutic targets for prostate cancer. *Oncogene* **41**, 3303–3315 (2022). doi: 10.1038/s41388-022-02347-1; pmid: 35568739

5. T. Wu et al., Recent developments in the biology and medicinal chemistry of CDK9 inhibitors: An update. *J. Med. Chem.* **63**, 13228–13257 (2020). doi: 10.1021/acs.jmedchem.0c00744; pmid: 32866383

6. B. Z. Stanton, E. J. Chory, G. R. Crabtree, Chemically induced proximity in biology and medicine. *Science* **359**, eaao5902 (2018). doi: 10.1126/science.aao5902; pmid: 29590011

7. P. M. Cromm, C. M. Crews, Targeted protein degradation: From chemical biology to drug discovery. *Cell Chem. Biol.* **24**, 1181–1190 (2017). doi: 10.1016/j.chembiol.2017.05.024; pmid: 28648379

8. C. M. Olson et al., Pharmacological perturbation of CDK9 using selective CDK9 inhibition or degradation. *Nat. Chem. Biol.* **14**, 163–170 (2018). doi: 10.1038/nchembio.2538; pmid: 29251720

9. G. E. Winter et al., DRUG DEVELOPMENT. Phthalimide conjugation as a strategy for in vivo target protein degradation. *Science* **348**, 1376–1381 (2015). doi: 10.1126/science.aab1433; pmid: 25999370

10. R. Schmitz et al., Genetics and pathogenesis of diffuse large B-cell lymphoma. *N. Engl. J. Med.* **378**, 1396–1407 (2018). doi: 10.1056/NEJMoa1801445; pmid: 29641966

11. E. Bal et al., Super-enhancer hypermutation alters oncogene expression in B cell lymphoma. *Nature* **607**, 808–815 (2022). doi: 10.1038/s41586-022-04906-8; pmid: 35794478

12. A. L. Shaffer et al., BCL-6 represses genes that function in lymphocyte differentiation, inflammation, and cell cycle control. *Immunity* **13**, 199–212 (2000). doi: 10.1016/S1074-7613(00)00020-0; pmid: 10981963

13. R. T. Phan, R. Dalla-Favera, The BCL6 proto-oncogene suppresses p53 expression in germinal-centre B cells. *Nature* **432**, 635–639 (2004). doi: 10.1038/nature03147; pmid: 15577913

14. K. Basso, R. Dalla-Favera, Roles of BCL6 in normal and transformed germinal center B cells. *Immunol. Rev.* **247**, 172–183 (2012). doi: 10.1111/j.1600-065X.2012.01112.x; pmid: 22500840

15. Y. Jiang et al., CREBBP inactivation promotes the development of HDAC3-dependent lymphomas. *Cancer Discov.* **7**, 38–53 (2017). doi: 10.1158/2159-8290.CD-16-0975; pmid: 27733359

16. N. Kerres et al., Chemically induced degradation of the oncogenic transcription factor BCL6. *Cell Rep.* **20**, 2860–2875 (2017). doi: 10.1016/j.celrep.2017.08.081; pmid: 28930682

17. O. A. Davis et al., Optimizing shape complementarity enables the discovery of potent tricyclic BCL6 inhibitors. *J. Med. Chem.* **65**, 8169–8190 (2022). doi: 10.1021/acs.jmedchem.1c02174; pmid: 35657291

18. B. R. Bellenie et al., Achieving in vivo target depletion through the discovery and optimization of benzimidazolone BCL6 degraders. *J. Med. Chem.* **63**, 4047–4068 (2020). doi: 10.1021/acs.jmedchem.9b02076; pmid: 32275432

19. S. Gourisankar et al., Rewiring cancer drivers to activate apoptosis. *Nature* **620**, 417–425 (2023). doi: 10.1038/s41586-023-06348-2; pmid: 37495688

20. G. S. Erwin et al., Synthetic transcription elongation factors license transcription across repressive chromatin. *Science* **358**, 1617–1622 (2017). doi: 10.1126/science.aan6414; pmid: 29192133

21. N. A. Hathaway et al., Dynamics and memory of heterochromatin in living cells. *Cell* **149**, 1447–1460 (2012). doi: 10.1016/j.cell.2012.03.052; pmid: 22704655

22. S. N. Ho, S. R. Biggar, D. M. Spencer, S. L. Schreiber, G. R. Crabtree, Dimeric ligands define a role for transcriptional activation domains in reinitiation. *Nature* **382**, 822–826 (1996). doi: 10.1038/382822a0; pmid: 8752278

23. N. Alerasool, H. Leng, Z. Y. Lin, A. C. Gingras, M. Taipale, Identification and functional characterization of transcriptional activators in human cells. *Mol. Cell* **82**, 677–695.e7 (2022). doi: 10.1016/j.molcel.2021.12.008; pmid: 35016035

24. R. N. Misra et al., N-(cycloalkylamino)acyl-2-aminothiazole inhibitors of cyclin-dependent kinase 2. N-[5-[[[5-(1,1-dimethylethyl)-2-oxazolyl]methyl]thio]-2-thiazolyl]-4-piperidinecarboxamide (BMS-387032), a highly efficacious and selective antitumor agent. *J. Med. Chem.* **47**, 1719–1728 (2004). doi: 10.1021/jm0305568; pmid: 15027863

25. T. Machleidt et al., NanoBRET—A novel BRET platform for the analysis of protein–protein interactions. *ACS Chem. Biol.* **10**, 1797–1804 (2015). doi: 10.1021/acschembio.5b00143; pmid: 26006698

26. M. Ghandi et al., Next-generation characterization of the Cancer Cell Line Encyclopedia. *Nature* **569**, 503–508 (2019). doi: 10.1038/s41586-019-1186-3; pmid: 31068700

27. K. Fujinaga et al., The ability of positive transcription elongation factor B to transactivate human immunodeficiency virus transcription depends on a functional kinase domain, cyclin T1, and Tat. *J. Virol.* **72**, 7154–7159 (1998). doi: 10.1128/JVI.72.9.7154-7159.1998; pmid: 9696809

28. Q. Li et al., Analysis of the large inactive P-TEFb complex indicates that it contains one 7SK molecule, a dimer of HEXIM1 or HEXIM2, and two P-TEFb molecules containing Cdk9 phosphorylated at threonine 186. *J. Biol. Chem.* **280**, 28819–28826 (2005). doi: 10.1074/jbc.M502712200; pmid: 15965233

29. K. Callaway, W. F. Waas, M. A. Rainey, P. Ren, K. N. Dalby, Phosphorylation of the transcription factor Ets-1 by ERK2: Rapid dissociation of ADP and phospho-Ets-1. *Biochemistry* **49**, 3619–3630 (2010). doi: 10.1021/bi100199q; pmid: 20361728

30. B. Lu, C. F. Wong, J. A. McCammon, Release of ADP from the catalytic subunit of protein kinase A: A molecular dynamics simulation study. *Protein Sci.* **14**, 159–168 (2005). doi: 10.1110/ps.04894605; pmid: 15608120

31. J. Shaffer, G. Sun, J. A. Adams, Nucleotide release and associated conformational changes regulate function in the COOH-terminal Src kinase, Csk. *Biochemistry* **40**, 11149–11155 (2001). doi: 10.1021/bi011029y; pmid: 11551213

32. K. V. Butler, A. M. Chiarella, J. Jin, N. A. Hathaway, Targeted gene repression using novel bifunctional molecules to harness endogenous histone deacetylation activity. *ACS Synth. Biol.* **7**, 38–45 (2018). doi: 10.1021/acssynbio.7b00295; pmid: 29073761

33. M. J. Dyer, P. Fischer, E. Nacheva, W. Labastide, A. Karpas, A new human B-cell non-Hodgkin's lymphoma cell line (Karpas 422) exhibiting both t (14;18) and t(4;11) chromosomal translocations. *Blood* **75**, 709–714 (1990). doi: 10.1182/blood.V75.3.709.709; pmid: 2297573

34. K. Hatzi *et al.*, A hybrid mechanism of action for BCL6 in B cells defined by formation of functionally distinct complexes at enhancers and promoters. *Cell Rep.* **4**, 578–588 (2013). doi: 10.1016/j.celrep.2013.06.016; pmid: 23911289

35. M. D. Gearhart, C. M. Corcoran, J. A. Wamstad, V. J. Bardwell, Polycomb group and SCF ubiquitin ligases are found in a novel BCOR complex that is recruited to BCL6 targets. *Mol. Cell. Biol.* **26**, 6880–6889 (2006). doi: 10.1128/MCB.00630-06; pmid: 16943429

36. C. Y. McLean *et al.*, GREAT improves functional interpretation of cis-regulatory regions. *Nat. Biotechnol.* **28**, 495–501 (2010). doi: 10.1038/nbt.1630; pmid: 20436461

37. J. Yu, Z. Wang, K. W. Kinzler, B. Vogelstein, L. Zhang, PUMA mediates the apoptotic response to p53 in colorectal cancer cells. *Proc. Natl. Acad. Sci. U.S.A.* **100**, 1931–1936 (2003). doi: 10.1073/pnas.2627984100; pmid: 12574499

38. R. J. Youle, A. Strasser, The BCL-2 protein family: Opposing activities that mediate cell death. *Nat. Rev. Mol. Cell Biol.* **9**, 47–59 (2008). doi: 10.1038/nrm2308; pmid: 18097445

39. L. Pasqualucci *et al.*, Mutations of the BCL6 proto-oncogene disrupt its negative autoregulation in diffuse large B-cell lymphoma. *Blood* **101**, 2914–2923 (2003). doi: 10.1182/blood-2002-11-3387; pmid: 12515714

40. H. Zhang *et al.*, Targeting CDK9 reactivates epigenetically silenced genes in cancer. *Cell* **175**, 1244–1258.e26 (2018). doi: 10.1016/j.cell.2018.09.051; pmid: 30454645

41. X. Liu *et al.*, Discovery of XL01126: A potent, fast, cooperative, selective, orally bioavailable, and blood-brain barrier penetrant PROTAC degrader of leucine-rich repeat kinase 2. *J. Am. Chem. Soc.* **144**, 16930–16952 (2022). doi: 10.1021/jacs.2c05499; pmid: 36007011

42. M. N. O'Brien Laramy, S. Luthra, M. F. Brown, D. W. Bartlett, Delivering on the promise of protein degraders. *Nat. Rev. Drug Discov.* **22**, 410–427 (2023). doi: 10.1038/s41573-023-00652-2; pmid: 36810917

43. K. Hatzi, A. Melnick, Breaking bad in the germinal center: How deregulation of BCL6 contributes to lymphomagenesis. *Trends Mol. Med.* **20**, 343–352 (2014). doi: 10.1016/j.molmed.2014.03.001; pmid: 24698494

44. B. H. Ye *et al.*, The BCL-6 proto-oncogene controls germinal-centre formation and Th2-type inflammation. *Nat. Genet.* **16**, 161–170 (1997). doi: 10.1038/ng0697-161; pmid: 9171827

45. D. Yu *et al.*, The transcriptional repressor Bcl-6 directs T follicular helper cell lineage commitment. *Immunity* **31**, 457–468 (2009). doi: 10.1016/j.immuni.2009.07.002; pmid: 19631565

46. A. L. Shaffer 3rd, R. M. Young, L. M. Staudt, Pathogenesis of human B cell lymphomas. *Annu. Rev. Immunol.* **30**, 565–610 (2012). doi: 10.1146/annurev-immunol-020711-075027; pmid: 22224767

47. A. L. Dent, A. L. Shaffer, X. Yu, D. Allman, L. M. Staudt, Control of inflammation, cytokine expression, and germinal center formation by BCL-6. *Science* **276**, 589–592 (1997). doi: 10.1126/science.276.5312.589; pmid: 9110977

48. C. Huang *et al.*, The BCL6 RD2 domain governs commitment of activated B cells to form germinal centers. *Cell Rep.* **8**, 1497–1508 (2014). doi: 10.1016/j.celrep.2014.07.059; pmid: 25176650

49. C. Huang, K. Hatzi, A. Melnick, Lineage-specific functions of Bcl-6 in immunity and inflammation are mediated by distinct biochemical mechanisms. *Nat. Immunol.* **14**, 380–388 (2013). doi: 10.1038/ni.2543; pmid: 23455674

50. A. L. Greenleaf, Human CDK12 and CDK13, multi-tasking CTD kinases for the new millenium. *Transcription* **10**, 91–110 (2019). doi: 10.1080/21541264.2018.1535211; pmid: 30319007

51. Z. Fan *et al.*, CDK13 cooperates with CDK12 to control global RNA polymerase II processivity. *Sci. Adv.* **6**, eaaz5041 (2020). doi: 10.1126/sciadv.aaz5041; pmid: 32917631

52. H. E. Kim *et al.*, Frequent amplification of CENPF, GMNN and CDK13 genes in hepatocellular carcinomas. *PLOS ONE* **7**, e43223 (2012). doi: 10.1371/journal.pone.0043223; pmid: 22912832

53. H. Liu, K. Liu, Z. Dong, Targeting CDK12 for cancer therapy: Function, mechanism, and drug discovery. *Cancer Res.* **81**, 18–26 (2021). doi: 10.1158/0008-5472.CAN-20-2245; pmid: 32958547

54. M. Ito *et al.*, Discovery of 3-Benzyl-1-(trans-4-((5-cyanopyridin-2-yl)amino)cyclohexyl)-1-arylurea Derivatives as Novel and Selective Cyclin-Dependent Kinase 12 (CDK12) Inhibitors. *J. Med. Chem.* **61**, 7710–7728 (2018). doi: 10.1021/acs.jmedchem.8b00683; pmid: 30067358

55. M. D. Galbraith, H. Bender, J. M. Espinosa, Therapeutic targeting of transcriptional cyclin-dependent kinases. *Transcription* **10**, 118–136 (2019). doi: 10.1080/21541264.2018.1539615; pmid: 30409083

56. S. Ding, Y. Rao, Q. Lu, Are BCL6 and EZH2 novel therapeutic targets for systemic lupus erythematosus? *Cell. Mol. Immunol.* **19**, 863–865 (2022). doi: 10.1038/s41423-022-00882-1; pmid: 35637283

57. X. Huang *et al.*, The expression of Bcl-6 in circulating follicular helper-like T cells positively correlates with the disease activity in systemic lupus erythematosus. *Clin. Immunol.* **173**, 161–170 (2016). doi: 10.1016/j.clim.2016.10.017; pmid: 27818202

58. S. U. Siriwardena *et al.*, Phosphorylation-inducing chimeric small molecules. *J. Am. Chem. Soc.* **142**, 14052–14057 (2020). doi: 10.1021/jacs.0c05537; pmid: 32787262

59. I. A. Graef, L. J. Holsinger, S. Diver, S. L. Schreiber, G. R. Crabtree, Proximity and orientation underlie signaling by the non-receptor tyrosine kinase ZAP70. *EMBO J.* **16**, 5618–5628 (1997). doi: 10.1093/emboj/16.18.5618; pmid: 9312021

60. C. Yu *et al.*, High-throughput identification of genotype-specific cancer vulnerabilities in mixtures of barcoded tumor cell lines. *Nat. Biotechnol.* **34**, 419–423 (2016). doi: 10.1038/nbt.3460; pmid: 26928769

61. S. M. Corsello *et al.*, Discovering the anti-cancer potential of non-oncology drugs by systematic viability profiling. *Nat. Cancer* **1**, 235–248 (2020). doi: 10.1038/s43018-019-0018-6; pmid: 32613204

62. K. Hatzi *et al.*, Histone demethylase LSD1 is required for germinal center formation and BCL6-driven lymphomagenesis. *Nat. Immunol.* **20**, 86–96 (2019). doi: 10.1038/s41590-018-0273-1; pmid: 30538335

63. Y. Perez-Riverol *et al.*, The PRIDE database resources in 2022: A hub for mass spectrometry-based proteomics evidences. *Nucleic Acids Res.* **50**, D543–D552 (2022). doi: 10.1093/nar/gkab1038; pmid: 34723319

ACKNOWLEDGMENTS

SUPPLEMENTARY MATERIALS

science.org/doi/10.1126/science.adl5361
Materials and Methods
Figs. S1 to S17
Tables S1 to S3
References (64–94)
MDAR Reproducibility Checklist